Spin-Resolved Unoccupied Electronic Band Structure from Quantum Size Oscillations in the Reflectivity of Slow Electrons from Ultrathin Ferromagnetic Crystals

R. Zdyb[1,2] and E. Bauer[1]

[1]*Department of Physics and Astronomy, Arizona State University, Tempe, Arizona 85287-1404*
[2]*Institute of Physics, Maria Curie-Sklodowska University, 20031 Lublin, Poland*

(Received 1 February 2002; published 3 April 2002)

The spin-dependent reflectivity of electrons with energies between 0 and 20 eV from Fe single crystals 2–8 monolayers thick on a W(110) surface is studied by spin-polarized low energy electron microscopy. The quantum size oscillations in the reflectivity are analyzed in a similar manner as in photoemission of ground state electrons, yielding the spin-resolved unoccupied state band structure of Fe in the ΓN direction in the energy range studied.

DOI: 10.1103/PhysRevLett.88.166403 PACS numbers: 71.20.Be, 68.37.Nq, 73.21.Fg, 75.30.Et

The electronic band structure is of fundamental importance for many solid state properties. Band structure calculations have reached a high level of sophistication, but the absolute positions of the bands, in particular of the unoccupied states, still need experimental verification. The band structure of ground states is usually determined by angle-resolved ultraviolet photoemission spectroscopy (ARUPS) [1]. This method has the problem that it involves two states, the initial (i) and the final (f) state, that cannot be determined simultaneously. This is so because there is no direct relation between the momentum of the emitted electron and the normal component $\mathbf{k}_{f\perp}$ of the excited electron, while the $\mathbf{k}$ component parallel to the surface is preserved during emission. Therefore $\mathbf{k}_f$ is not fully known and consequently also not $\mathbf{k}_i$. The problem is usually solved by either assuming a free electronlike final state or by taking the final state from band structure calculations that are known to have considerable uncertainty, in particular in materials with wide band gaps. In addition, if the material has a high density of unoccupied states or when the final states are above the plasmon excitation threshold, then the inelastic mean free path Λ of the electron is short. This leads to an uncertainty of $\mathbf{k}_{f\perp}$ that makes a range of final states accessible with the corresponding uncertainty in the initial state $\mathbf{k}_{i\perp}$ [2].

These problems can be avoided only if $\mathbf{k}_{i\perp}$ is determined independently from the emission process. If the electron system is confined to a thin slab with thickness t, then the boundary conditions require that the wave functions must have nodes at the boundaries so that $n\lambda/2 + \varphi = t$ or $kt - \Phi = n\pi$, where n is an integer, λ is the wavelength, φ takes account of the finite penetration of the wave beyond the boundaries and of their imperfect reflectivity, and $\Phi = k\varphi$ is the phase shift at the two boundaries of the slab. Thus $\mathbf{k}_\perp$ is determined by the boundary conditions. These boundary conditions produce the well-known quantum well states that have been observed first in low energy electron transmission [3] and studied thereafter with a variety of techniques such as electron tunneling [4], low energy reflection [5], photoemission [6], high energy electron reflection, and electrical resistivity measurements [7]. A recent review of the photoemission work demonstrates the power of quantum well studies for the determination of the ground state band structure [8]. Mainly thanks to photoemission studies in general the occupied state band structure of many materials is now experimentally well established.

Much less is known from experiment about the unoccupied state band structure. Inverse photoemission, in particular in quantum wells [9], has been used to determine the band structure of unoccupied states below the vacuum level, but little is known from experiment about the band structure above the vacuum level. In this Letter we report a quantum well study of the unoccupied state band structure of Fe using the reflection of slow polarized electrons from ultrathin Fe microcrystals with well-defined thickness. In this and other ferromagnetic materials the bands are split into spin-up and spin-down bands by the exchange interaction. This makes them not only important because of their ground state properties but also opens up interesting applications based on their unoccupied state properties, such as in spin polarizers and analyzers. For this application the exchange splitting is of fundamental importance. At the band edges it can produce a very high figure of merit $Q = A^2 I/I_0$ of these devices where $A = (I_\uparrow - I_\downarrow)/(I_\uparrow + I_\downarrow)$ is the "asymmetry" of the reflected current of spin-up ($I_\uparrow$) and spin-down ($I_\downarrow$) electrons and I_0 is the incident current. For example, on Fe(100) surfaces a Q value of 3.5×10^{-3} has been observed at the H_{12} point [10]. On Fe(110) a Q value of 8×10^{-3} has been measured at 5 eV [11], an energy that corresponds to the N_1 point. In quantum wells the quantization conditions are fulfilled for different energies for spin-up and spin-down electrons due to the exchange splitting. This causes considerable enhancements of A at low energies. For example, in 5 monolayer (ML) thick Co films on W(110) a Q value of 2×10^{-2} was obtained at 2 eV [12] and the ultrathin Fe (110)-oriented Fe crystals on W(110) used here for band structure analysis gave Q values of 5×10^{-2} [13]. These values are 2 orders of magnitude larger than those of conventional spin polarimeters. Thus,

the unoccupied state band structure in ferromagnetic materials is not only important for the determination of the ground state band structure via ARUPS but also of practical importance.

The experiments were performed *in situ* in a spin-polarized low energy electron microscope (SPLEEM) that has been described elsewhere in more detail [14,15]. A nearly parallel beam of slow electrons with normal incidence on the sample is produced by focusing a spin-polarized 15 kV electron beam into the back focal plane of a cathode lens. In this lens the electrons are decelerated to the desired energy at the sample, reaccelerated again after reflection, and used for imaging the surface, typically 2500–10 000 times. This high magnification is necessary in order to be able to measure the intensity reflected from microcrystals. The electron beam with a degree of polarization $P \approx 0.2$ was produced by illuminating a GaAs (100) surface, activated with Cs and O_2 to negative electron affinity, with circular polarized light from a diode laser. The polarization vector **P** of the electrons could be rotated in any desired direction with a magnetic/electrostatic deflector and a rotator lens [16]. In the present experiment in which the sample has uniaxial magnetic anisotropy, that is domains with only two magnetization directions ($\mathbf{M}, -\mathbf{M}$), it was sufficient to change **P** by changing the helicity of the circular polarized light with a Pockels cell.

The W crystal was cleaned in the usual way by alternating heating in O_2 at around 1400 K with flashing off the oxygen remaining after removal of C, S, and other impurities at about 2000 K. This procedure results in a considerable surface rearrangement into large atomically flat terraces up to 10 μm in diameter and regions with high step density and step bunches. The large terraces were used for the study of the Fe microcrystals grown on them. Fe was deposited from a boron nitride crucible at a grazing angle of incidence of 16° at temperatures ranging from 300 to 900 K at a rate of about 2×10^{-3} ML/sec at a pressure below 3×10^{-10} Torr, the base pressure being in the upper 10^{-11} Torr range. The growth was monitored with SPLEEM that allowed selection of the best conditions for the growth of atomically flat Fe crystals. The crystals grew via the Stranski-Krastanov mode over several terraces that resulted in μm large regions with constant thickness, varying from terrace to terrace (see, for example, Fig. 1).

After deposition the sample was cooled to room temperature and images with opposite **P**, that is, spin-up and spin-down images at fixed **M**, were taken as a function of energy in 0.2 eV energy steps. Areas of typically 1 μm^2 were selected for the intensity measurements in the images that were acquired with a charge-coupled device camera. At energies $E < 0$, that is, in the mirror mode, all electrons are reflected so that the intensities below $E = 0$ are a measure for I_0. The intensities I at energies $E > 0$ are normalized to I_0, both for spin-up and spin-down images to give the reflectivities $R_\uparrow$ and $R_\downarrow$. Figure 2 shows

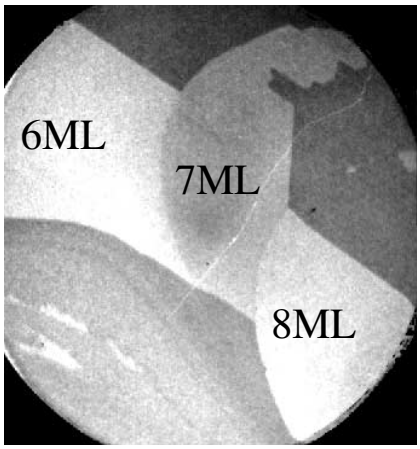

FIG. 1. LEEM image of an Fe(110) microcrystal ranging from 6 (upper left) to 8 (lower right corner) monolayers in thickness on a terraced W(110) surface. Energy 11.4 eV, diameter of field of view 9 μm. The SPLEEM (asymmetry) images show much better contrast but can be presented usefully only in color (see, e.g., Ref. [13]).

a few selected $I_\uparrow(E)/I_0 = R_\uparrow(E)$ curves. The peak at around 21 eV is the (220) reflection from Fe, but between this peak and the rapid change near 0 eV weak quantum size oscillations are seen. Before these data can be used for the determination of the spin-dependent band structure they have to be corrected for the degree of polarization. With $P = 20\%$ the remaining 80% of the current consists of half spin-up and spin-down electrons. This correction yields $R_{c\uparrow} = 3R_\uparrow - 2R_\downarrow$ for the spin-up reflectivity corrected for 100% polarization and a corresponding relation for the spin-down reflectivity. Next the energy-dependent zero line around which the intensity oscillates has to be subtracted. It is obtained by measuring the intensity reflected from a thick crystal or a thick layer which shows no oscillations and scaling it to the (220) peak of the thinner crystals. The result is illustrated in Fig. 3 for a 6 ML thick crystal for both spin-up and spin-down reflectivities. The displacement of the peak positions due to the exchange splitting and the resulting differences in the energies at which the quantization condition is fulfilled is clearly visible. The smaller amplitude of the spin-down oscillations is a consequence of the significantly shorter inelastic mean free path of the spin-down electrons compared to that of the spin-up electrons (see, for example, [17,18]).

The data in Fig. 3 can now be analyzed in a manner similar to that used in UPS. The energies of the extrema of the oscillations are plotted as a function of thickness as shown in Fig. 4 for the spin-up case. The points at different thicknesses with the same quantum number are connected by thin lines. The unknown phase $\Phi(E)$ in the quantization condition $k(E)t - \Phi(E) = n\pi$ can be eliminated by choosing energies at which the condition is fulfilled for two (t, n) pairs. From these pairs one obtains $k(E) = \pi \times (n_2 - n_1)/(t_2 - t_1)$ for these energies. The experimental data are limited to 3–8 ML because the first

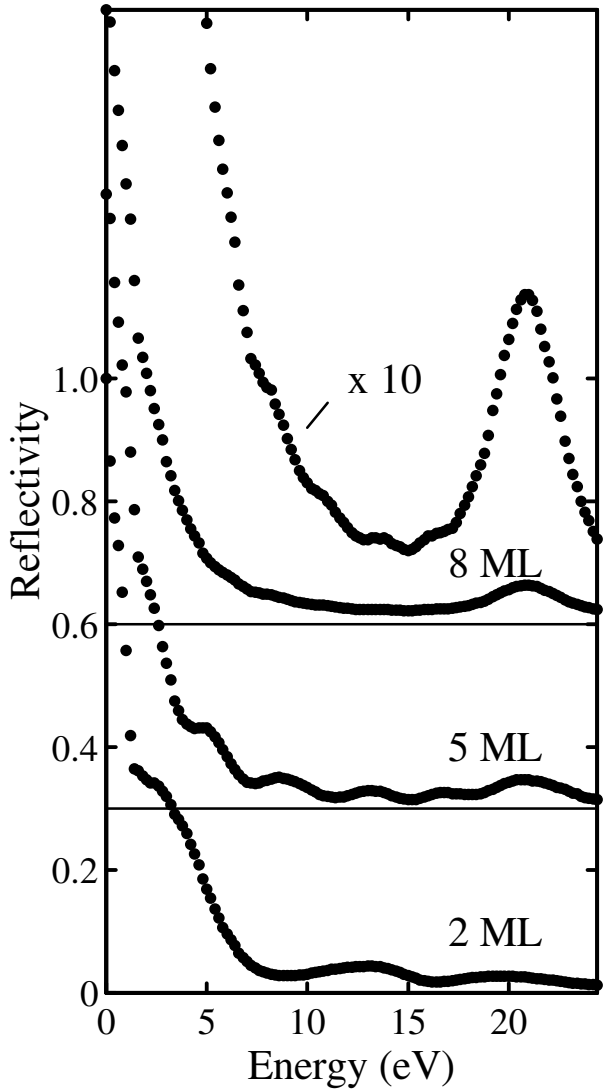

FIG. 2. Spin-up reflectivity of 2, 5, and 8 ML thick Fe(110) microcrystals as a function of energy. The curves have been displaced by 0.3 for better visibility.

2 ML do not have the Fe(110) structure and above 8 ML the oscillations are too weak due to the short inelastic mean free path in Fe. The energy range is limited to 5–20 eV because below 5 eV it is difficult to extract the oscillations from the rapidly varying background and above 20 eV the amplitudes are too weak, again because of the short inelastic mean free path. Therefore not only maxima but also the minima for which n is replaced by $(2n + 1)/2$ were analyzed. $k(E)$ is in this case given by the same condition as for the maxima while for the maxima-minima pairs $n_2 - n_1$ is replaced by $n_2 - n_1 - 1/2$. The corresponding horizontal lines are shown in Fig. 4 and the $k(E)$ pairs both for spin-up and spin-down electrons in the usual $E(k)$ plot in Fig. 5. For comparison the results of two band structure calculations are shown as solid [19] and dotted [20] curves, assuming a work function of 4.85 eV. The experimental data agree well with the solid curve except

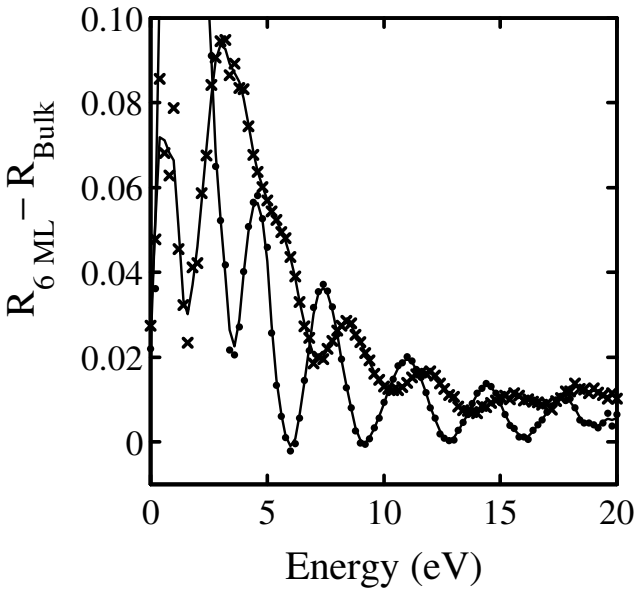

FIG. 3. Spin-up (•) and spin-down (×) reflectivity difference between a 6 ML thick and a very thick ("bulk") Fe(110) crystal after correction for the degree of polarization as a function of energy.

for the points in the middle of the Brillouin zone. Careful reexamination of all data showed that this deviation is systematic. It could be due to a zone boundary that would indicate a doubling of the periodicity normal to the surface. Oscillations of the interlayer spacing, of the electron density, or of the spin alignment could cause such a periodicity, but in the absence of experimental points just below the center of the Brillouin zone this remains an open question. A two-band fit to the data points gives an exchange

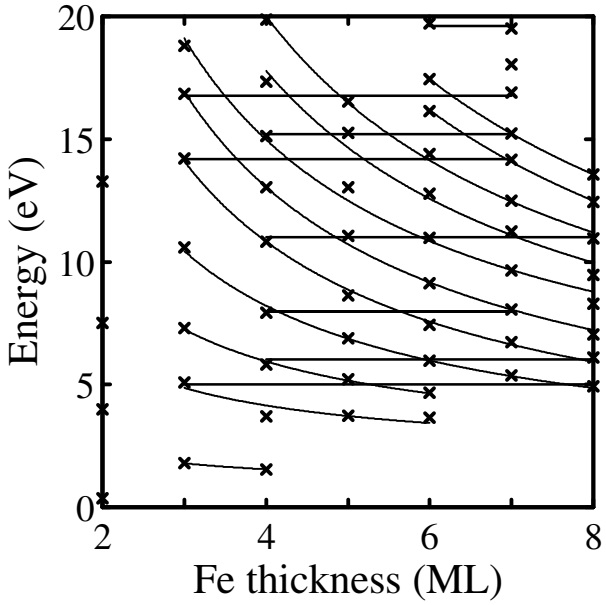

FIG. 4. Energy positions of the extrema of the spin-up reflectivity oscillations in 2–8 ML thick Fe(110) microcrystals. For explanation, see the text.

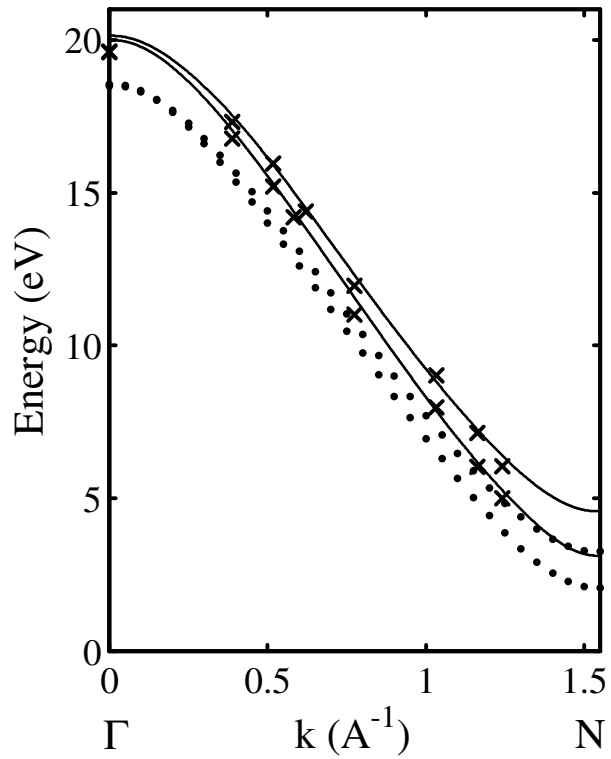

FIG. 5. $E(k)$ values derived from the data of Fig. 4 (crosses) and calculated band structures from Ref. [19] (solid curves) and Ref. [20] (dotted curves) along the ΓN direction of Fe.

splitting at the N of 1.26 eV in between the theoretical values of 1.36 eV [19] and 1.19 eV [20].

It is interesting to note that the upper curve agrees better with experiment than the lower one although the upper is calculated with the full-potential linearized augmented plane wave (FLAPW) method while the lower one used the APW method that is believed to be better suited than the linearized method [19,20]. On the other hand, another FLAPW calculation [21] gives a band structure similar to the APW calculation, at least in the ΓH direction. All three calculations use the same exchange-correlation potential. Thus, differences in the computational details seem to plan an equally important role. Additional support for the band structure of Ref. [19] comes from a recent inverse photoemission, reflected and absorbed current study of a thick Fe(100) film [22]. In this study the results were compared with still another band structure calculation [23] that gives H_{15} and H_{12} energies close to those of Ref. [20]. A comparison with the band structure of Ref. [19], however, gives a much better fit: the exchange-split inverse photoemission peak is located exactly at the energy of the exchange-split band edge at H_{15}; the maximum reflectivity is exactly in the center of the band gap between H_{15} and H_{12} and also the asymmetries of the reflected and the absorbed current agree well with the band structure of Ref. [19].

Summarizing, we have determined the exchange-split band structure of Fe in the ΓN direction above the vacuum level from the quantum size oscillations of the spin-dependent reflectivity of 3–8 ML thick Fe microcrystals on a W(110) surface. These measurements became possible by optimizing the growth of these microcrystals *in situ* in a spin-polarized low energy electron microscope. The results allowed us to distinguish between different band structure calculations and are of fundamental importance for the design of spin polarizers and analyzers.

We thank K. B. Hathaway and D. A. Papaconstantopoulos for their band structure data. This material is based on work supported by the National Science Foundation under Grant No. 9818296.

[1] S. Huefner, *Photoelectron Spectroscopy* (Springer, Berlin, 1995).
[2] M. Jalochowski *et al.,* Phys. Rev. B **46**, 4963 (1992).
[3] R. F. Thomas, J. Appl. Phys. **41**, 5330 (1970).
[4] R. C. Jaklevic *et al.,* Phys. Rev. Lett. **26**, 88 (1971).
[5] R. C. Jaklevic, Phys. Rev. B **30**, 5494 (1984).
[6] A. L. Wachs *et al.,* Phys. Rev. B **33**, 1460 (1986).
[7] M. Jalochowski and E. Bauer, Phys. Rev. B **38**, 5272 (1988).
[8] T.-C. Chiang, Surf. Sci. Rep. **39**, 181 (2000).
[9] F. J. Himpsel, Phys. Rev. B **44**, 5966 (1991).
[10] D. Tillman, R. Thiel, and E. Kisker, Z. Phys. B **77**, 1 (1989).
[11] G. Fahsold *et al.,* Solid State Commun. **84**, 541 (1992).
[12] K. Wurm, M.S. thesis, TU Clausthal, 1994.
[13] R. Zdyb and E. Bauer, Surf. Rev. Lett. (to be published).
[14] E. Bauer, in *Handbook of Microscopy, Methods II,* edited by S. Amelinckx *et al.* (VCH, Weinheim, 1997), p. 751.
[15] T. Duden and E. Bauer, J. Electron Microsc. **47**, 379 (1998).
[16] T. Duden and E. Bauer, Rev. Sci. Instrum. **66**, 2861 (1995).
[17] H.-J. Drouhin, Phys. Rev. B **62**, 556 (2000).
[18] J. Hong and D. Mills, Phys. Rev. B **62**, 5589 (2000).
[19] K. B. Hathaway, H. J. F. Hansen, and A. J. Freeman, Phys. Rev. B **31**, 7603 (1985).
[20] D. A. Papaconstantopoulos (private communication).
[21] J. Noffke, referenced in Ref. [11].
[22] R. Bertacco and F. Ciccacci, Phys. Rev. B **59**, 4207 (1999).
[23] E. Tamura and R. Feder, Phys. Rev. Lett. **57**, 759 (1986).